Stereoelectronic Effects in Pentacoordinate Intermediates and Acceleration of Nucleophilic Substitution at Phosphorus

Gregory R. J. Thatcher,* E. S. Krol and Dale R. Cameron
Department of Chemistry, Queen's University, Kingston, Ontario, Canada K7L 3N6

Hydroxide-dependent hydrolysis of triesters of phosphonoformic acid (PFA) *via* P–O bond cleavage proceeds at rates 10^3–10^6 times greater than hydrolysis of simple phosphonates. The means by which an α-carbonyl substituent elicits such a rate enhancement has been examined using *ab initio* calculations. Model compounds have been derived, from full geometry optimization at the RHF/6-31G*//6-31G* level, of (*a*) the tetracoordinate ground state PFA triesters (**4**, RPO_3Me_2; R = CHO) and simple phosphonate esters (**4**, R = CF_2H, CH_3), and (*b*) pentacoordinate intermediates for hydrolysis of these triesters (**5**, $RPO_4H_3^-$; **6**, $RPO_4HMe_2^-$, R = CHO, CO_2H and **5**, **6**, R = CF_2H, CH_3, respectively). Intramolecular charge-transfer interactions have been quantified employing natural bond orbital analysis, including calculation of molecular energies on deletion of each individual interaction. These molecular orbital calculations demonstrate significant stabilizing, intramolecular charge-transfer interactions, including internal hydrogen bonding and $n_p(O)\rightarrow\pi^*(C{=}O)$ charge transfer in the pentacoordinate state. The $n\rightarrow\pi^*$ stabilization contributes 4–10 kcal mol^{-1} to the stabilization of these intermediates in the gas phase. It is suggested that such charge-transfer stabilization in the pentacoordinate intermediates and transition states for hydrolysis of PFA triesters contributes to the observed rate enhancement. In contrast, these calculations show no evidence for the stereoelectronic effect (akin to the generalized anomeric effect) proposed by Gorenstein and Taira for pentacoordinate phosphoranes and suggested also to lead to large rate enhancements for nucleophilic substitution at phosphorus. Calculations on models [**7**, $RC(O)CO_3HMe^-$, R = H, OH] for tetrahedral intermediates in oxalate ester hydrolysis demonstrate a greatly diminished intramolecular $n_p(O)\rightarrow\pi^*(C{=}O)$ charge-transfer stabilization. This is in accord with rate data on carboxylate ester hydrolysis.

It has been said that phosphate esters dominate the living world.[1] The process of making and breaking phosphate ester bonds is a fundamental biological reaction and of particular current interest in development of antisense and antigene therapeutic strategies.[2] Although biomolecules have been isolated, possessing a phosphonate rather than phosphate functionality,[3] the major interest in phosphonates has been associated with their function as insecticides and nerve agents,[4] where degradation by P–O bond cleavage is of clear importance. The reaction in question is nucleophilic substitution at phosphorus and factors which lead to acceleration of this reaction are of major interest and the subject of intensive study.[5,6] The rate of P–O bond cleavage in the hydrolysis of phosphonoformate triesters (**1**) has been observed to be enhanced a millionfold relative to simple phosphonates (**2a,b**) and to occur 10^3–10^5 more rapidly than an activated phosphonate (**3**).[7] A possible rationale for the greatly enhanced reactivity of α-carbonyl phosphonates has its origin in stereoelectronic interactions. In order to examine this rationale, stereoelectronic effects in the pentacoordinate intermediates for hydrolysis of a series of phosphonate esters have been quantified employing *ab initio* molecular-orbital calculations.

Evidence for the presence of stereoelectronic effects in ground-state tetracoordinate phosphoryl species, compatible with the generalized anomeric effect,[8] has been provided by solid-state crystallography and solution NMR spectroscopy.[9] Early calculations by Lehn and Wipff provided a basis for the presence of such effects in theory using conformational energy, geometry and Mulliken population analysis as indicators,[10] although the precise origin of such effects in electrostatic, hyperconjugative or other charge-transfer interactions remains to be defined. Analysis of the individual interactions contributing to stereoelectronic effects is aided by the localization of molecular orbitals on molecular fragments. To this end, Weinhold's natural bond orbital (NBO) analysis[11] has been used effectively in studies on the anomeric effect, particularly by Schleyer's group in identifying contributions from hyperconjugation.[12] Stereoelectronic effects in pentacoordinate phosphoranes have been proposed by Trippett[13] and in recent calculations performed by Streitwieser and Schleyer.[14] But by far the largest body of published work is that due to Gorenstein[15] and latterly Taira.[16] Using molecular-orbital calculations, but without analysis of interaction energies of specific localized molecular orbitals, these workers proposed a stereoelectronic effect, analogous to a generalized anomeric effect at pentacoordinate phosphorus. Again, in analogy with the kinetic anomeric effect[17] (or antiperiplanar lone-pair hypothesis)[18] the Gorenstein–Taira (GT) effect on transition-state energy has been translated into a predicted rate enhancement for nucleophilic substitution at phosphorus of enormous magnitude. Despite the lack of experimental evidence to support this conclusion,[5,19,20] large enhancements of rates for phosphoryl transfer processes, for example in nucleic acid cleavage, continue to be attributed to the GT effect.[16b] The search for factors leading to stereoelectronic acceleration is inspired by observations of unexplained rate phenomena. To some extent invocation of the GT effect was rationalized by

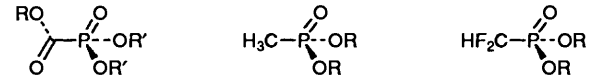

1a; R = Et, R′ = Et
b; Ar, R′ = Et
c; Et, R′ = Ph

2a; R = Et
b; Ph

3; R = Et

* Fax 613-545-6669; Tel. 613-545-2640.

the 10^5–10^8 fold rate enhancement observed for hydrolysis of five-membered ring phosphates.[5,19,20]† The comparable, rapid rate observed for hydrolysis of phosphonoformate triesters at neutral pH provides another such phenomenon. The *ab initio* calculations presented herein, employing quantitative NBO analysis, provide a stereoelectronic explanation for the observed enhanced reactivity of α-carbonyl phosphonates, but a contraindication of the existence of the GT effect.

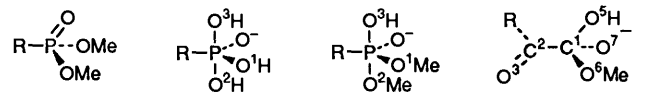

4a; R = CHO **5a**; R = CHO **6a**; R = CHO **7a**; R = H
b; CF_2H **b**; CF_2H **b**; CF_2H **b**; O^4H
c; CH_3 **c**; CH_3 **c**; CH_3
d; CO_2H **d**; CO_2H **d**; CO_2H

Methodology

The energy and structure of model compounds **4**–**7** was calculated employing full geometry optimization at the RHF/6-31G*//6-31G* level using GAUSSIAN 92 on IBM RISC 6000/320E or 355 using the standard basis set supplied by Gaussian.[23] Pre-orthogonal NBO overlap matrices were obtained and second-order perturbational analyses and full NBO analyses performed with GAUSSIAN 92. Mulliken charges and charges derived from the electrostatic potential (CHELPG) were recorded for each structure.[24] The identity of stationary points was confirmed by calculation of analytical frequencies. Structures for the α-carbonyl hemiorthoesters **7a,b** were located by full geometry optimization (6-31G*), including full NBO analysis and calculation of charge-transfer interaction energies. Exploration of torsional profiles was performed using SPARTAN 2.1[25] on an SGI Iris Indigo, in some cases at the RHF/3-21+G(*)//3-21+G(*) level.[26] A fixed rotor torsional scan (energy point calculations with no geometry optimization) was performed for P–C bond rotation on phosphorane **8** and a torsional scan with full optimization performed for P–C bond rotation of **6a** (starting geometries were obtained from full optimization at RHF/6-31G*//6-31G*). Calculations on $HC(O)PH_4$ used the 6-31G* basis set. Halophosphoranes **9a,b** were studied by full optimization at two different XP–CO torsion angles, using the 3-21+G(*) (**9b**) and 3-21G(*) and 6-31G* (**9a**) basis sets. Arguments on the requirement for large basis sets, diffuse and polarization functions for calculations on phosphoryl species have been discussed.[27] It was recently stated that the 6-31G* basis set was adequate for calculations on phosphate monoanions.[28]

Results

Rotational Profiles and Conformational Energy.—Geometry optimization of phosphorane **8** (6-31G*) yields a distorted trigonal bipyramidal (TBP) structure, with the methoxy group apical and the carbonyl moiety at the equatorial position and lying somewhat out of the equatorial plane [$\theta = \tau\{OCPO(H)\} = 67°$]. A rigid rotor torsional scan on rotation about the P–C bond shows barriers to rotation in both directions (Fig. 1). At torsion angles of 84.2°, 0.5° and 151.2° the energy increase is 0.6, 6.9 and 10.3 kcal mol^{-1}, respectively. A rotational energy profile for phosphorane **6a** was obtained

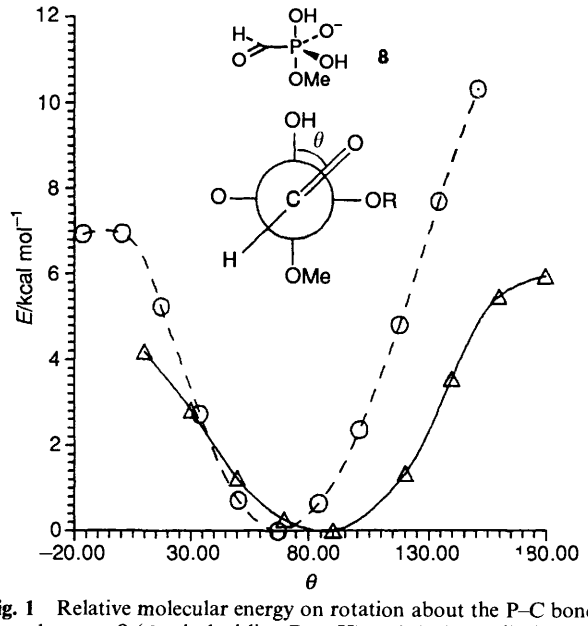

Fig. 1 Relative molecular energy on rotation about the P–C bond of phosphoranes **8** (○, dashed line R = H) and **6a** (△, solid line, R = Me). Calculations for **8** from fixed rotor scan, using point calculations at RHF/6-31G*//6-31G*; calculations for **6a** by full geometry optimization at each torsion angle.

by full geometry optimization at a series of fixed P–C bond torsional angles, using, as the starting geometry, the minimum energy conformer with the carbonyl moiety in the equatorial plane. Again, rotation of the carbonyl moiety from the equatorial to axial plane was accompanied by an energy increase, in this system, of 4–6 kcal mol^{-1} (Fig. 1). The destabilization as τ increases may partly reflect the steric influence of the apical methoxy ligand. In an attempt to reduce the contribution of steric effects, the simple phosphorane $HC(O)PH_4$ was studied. However, no stationary point could be located in which the carbonyl moiety occupied the equatorial position in a TBP. Instead, in the located stationary point (6-31G*), the carbonyl ligand was found at the apical position.

Stationary points were found for dichlorophosphorane **9a**, at the 3-21G(*) and 6-31G* levels, with the carbonyl moiety in the equatorial position of a TBP. Two conformers, with the carbonyl moiety either in the apical or equatorial plane, were located by full optimization. Calculation of analytical frequencies at the HF/6-31G* level demonstrated both conformers to be transition states, possessing one imaginary frequency in each case. The conformational space was not explored further. In addition, two rotamers of difluorophosphorane **9b** were obtained by full optimization using the 3-21+G(*) basis set, those conformers with the formyl group in the apical plane being lower in energy (Scheme 1).

Tetrahedral and Pentacoordinate Ground States.—Tetrahedral ground state structures were located for **4a–d** (6-31G*) and selected structural data are presented together with charges at atoms derived from Mulliken population analysis and electrostatic potentials (CHELPG) (Table 1). Compounds **4a–d** model the ground state reactants (**1**, **2**, **3**) for these processes. The charges at the electrophilic sites and scissile bond lengths of the ground-state tetrahedral species do not indicate any linear correlations with polar effects of substituents. Indeed the correlation between trends in Mulliken-derived charges and charges from electrostatic potentials is poor in itself (Table 1). Addition of hydroxide to **4a–d** yields the pentacoordinate structures **6a–d**. Phosphoranes **5a–d** represent simpler models of the pentacoordinate intermediates.

† Relief of ring strain in the pentacoordinate state is generally provided as the rationale for the enhanced reactivity of five-membered cyclic phosphates. However, a quantitative discrepancy between rate enhancements and estimates of relief of ring strain has been noted.[21] Various alternative explanations have been suggested, without reference to stereoelectronic effects.[22]

Table 1 Charges at atoms [electrostatic charges (CHELPG) and Mulliken], bond lengths, and molecular energy (hartree, E_h) for tetracoordinate phosphonate ester ground states **4a–d**

		4a	**4b**	**4c**	**4d**
Charge on carbonyl C	CHELPG	+0.319	+0.215	+0.152	+0.598
	Mulliken	+0.53	+0.379	−0.178	+0.490
Charge on P	CHELPG	+1.165	+1.080	+1.369	+1.229
	Mulliken	+1.496	+1.492	+1.538	+1.512
Bond length	*d*(P-C)/Å	1.838	1.834	1.795	1.846
	d(P-OMe)/Å	1.573, 1.573	1.575, 1.569	1.594, 1.581	1.571,1.566
Molecular energy	RHF/6-31G*//6-31G*	−757.885 322	−881.910 523	−684.221 345	−8 32.776 148

Table 3 Comparison of calculated molecular energies on deletion of charge-transfer interactions from NBO analysis, for α-carbonyl (**5a**, **6a**) and difluoromethyl (**5b**, **6b**) phosphoranes

			ΔE/kcal mol^{-1}		
	Donor[a]	Acceptor[a]	**5b–5a**	**6b–6a**	Description
Remote	nO (apical)	C=O/CF_2H	+3.93	+5.42	n(O)→π* (C=O)
	nO (apical)	σ*(Oeq-H)	−1.18	—	hydrogen-bonding
Geminal	eq. bonding	ap. antibond	+2.59	−2.04	
	ap. bonding	eq. antibond	−3.70	+1.81	
	ap. bonding	ap. antibond	+1.44	+0.74	
	eq. bonding	eq. antibond	−1.04	−0.06	
	P-C bonding	C=O/CF_2H	−0.092	0.0	
Vicinal	ap. bonding	eq. ligands	+2.12	+1.67	
	nO (apical)	eq. antibond	−1.45	−5.98	
	nO (apical)	ap. antibond	+0.30	−0.48	
	nO (eq. ether)	σ*(Oap-H) ap.	+0.42	+0.13	GT effect
	nO (eq. ether)	other antibond	−0.53	+0.70	
	nO (oxyanion)	all antibond	+0.42	−0.18	
	(O–H) eq. bond	all antibond	−0.98	+0.04	
	(O–H) ap. bond	all antibond	−0.27	−0.44	

[a] n = non-bonding; antibond = σ* + π*; bond = σ + π: eq. = equatorial; ap. = apical.

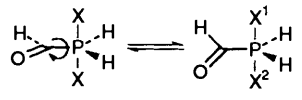

9a: X = Cl E = 0.01 0 kcal mol^{-1} [3-21G(*)]
E = 0.0 1.06 kcal mol^{-1} [6-31G* + E_{ZP}]
b: X = F E = 0.97 0 kcal mol^{-1} [3-21G(*)]

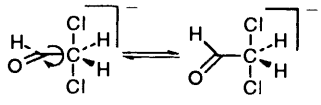

E = 0 11 kcal mol^{-1} [4-31G (ref. 36)]

Scheme 1

Natural Bond Orbital Analysis.—Two levels of NBO analysis were carried out on the wavefunctions derived for phosphoranes **5a–d**, **6a–d** and **9a**. Second-order perturbational molecular-orbital calculations yield the stabilization energies for pairwise interactions of localized non-bonding atomic and bond orbitals (Fig. 2, Table 2; selective structural parameters are also included). Independent recalculation of molecular energy was performed on deletion of each pairwise interaction for **5a,b** and **6a,b**. The character of each atomic orbital and identity of each bond orbital is included within the NBO analysis. However, a large number of substantial charge-transfer interactions are indicated in each compound, in particular deriving from geminal interactions. Correlation and comparison of interaction and deletion energies for the congener pairs **5a**/**5b** and **6a**/**6b** is necessary to define significant charge-transfer interactions present in the formyl and absent in the difluoromethyl derivative and *vice versa*. These are summarized in Table 3 showing that the only significant interaction leading to stabilization, common between both pairs of compounds examined, is the remote n(O)→π*(C=O) interaction.

Hemiorthoesters.—The hemiorthoesters **9a,b** are models of tetrahedral intermediates in oxalate ester hydrolysis, located by full geometry optimization (6-31G*). NBO analysis has again been used to provide pairwise charge-transfer interaction energies. Selected interactions and structural features are included in Table 4 for comparison with data on the pentacoordinate intermediates (Table 2 and Fig. 2).

Discussion

Hydrolysis of Phosphonoformate Triesters.—Hydrolysis of PFA triesters in the region pH > 6.5 is hydroxide-dependent.[7a] Reaction leads to P–C bond cleavage giving hydrogen phosphonates or P–O bond cleavage (Scheme 2) to yield the PFA diester monoanion **10**.[7b] The ratio of P–O to P–C bond cleavage products is dependent on pH, buffer concentration and leaving group ability. Thus for the *P*-phenoxy ester, exclusive P–O bond cleavage is observed, whereas for the *P*-ethoxy esters, P–C cleavage is competitive. Comparison of rate data for P–O bond cleavage with data for hydroxide-dependent hydrolysis of simple phosphonates demonstrates a rate enhancement of 10^3–10^6 for the α-carbonyl phosphonates.[7a] The observation, on

Table 2 Selected geometrical parameters, molecular energies (hartree, E_h) and pairwise charge-transfer interactions from NBO analysis (kcal mol^{-1})[a] for pentacoordinate phosphoranes **5a–d**, **6a–d** and dichlorophosphorane **9a**

	5a	**5b**	**5c**	**5d**	**6a⊥**[b]	**6b**	**6c**	**6d**	**6a∥**[b]		**9a⊥**[b]	**9a∥**[b]
d(P–O^1)/Å	1.622	1.626	1.643	1.620	1.631	1.642	1.655	1.630	1.648	d(P–Cl^1)/Å	2.193	2.266
d(P–O^2)/Å	1.709	1.694	1.720	1.707	1.722	1.709	1.747	1.718	1.698	d(P–Cl^2)/Å	2.193	2.122
d(P–O^3)/Å	1.797	1.808	1.817	1.780	1.761	1.764	1.768	1.748	1.766	d(P–H)/Å	1.370	1.371
d(P–C)/Å	1.839	1.865	1.838	1.856	1.845	1.881	1.841	1.861	1.900	d(P–C)/Å	1.371	1.371
d(C=O)/Å	1.194	—	—	1.194	1.193	—	—	1.194	1.190	d(C=O)/Å	1.174	1.167
∠CPO^2	87.83	91.59	89.90	86.57	83.32	84.27	86.32	82.08	86.28	∠CPCl^1	90.20	87.48
∠CPO^3	83.26	84.44	86.04	83.92	82.46	84.49	85.63	82.73	83.13	∠CPCl^2	90.20	95.63
∠RCO	119.30	—	—	119.57	119.37	—	—	119.69	119.28	∠RCO	124.93	126.06
τHO^{1}PO^3	−4.78	−4.47	−6.75	−4.27	—	—	—	—	—	—	—	—
τCO^{1}PO^2	—	—	—	—	−169.11	−165.48	−160.21	−170.32	−163.70	—	—	—
Energy/E_h	−755.2818	−879.3027	−681.5906	−830.1736	−833.3206	−957.3381	−759.6290	−908.2119	−833.3111		−1374.1265	−1374.1251
$n_pO^2 \rightarrow \pi^*$(C=O)	4.79	—	—	5.79	4.67	—	—	5.23	σ*(2.3)[c]	$n_pCl^1 \rightarrow \pi^*$(C=O)	3.70	σ*(1.5)[c]
$n_pO^3 \rightarrow \pi^*$(C=O)	7.24	—	—	6.33	8.02	—	—	7.28	σ*(0.5)[c]	$n_pCl^2 \rightarrow \pi^*$(C=O)	3.72	σ*(0.5)[c]
$n_pO^2 \rightarrow$BD*(R group)	—	2.41	0	—	—	1.46	0.52	—	—	$n_pCl^2 \rightarrow \sigma^*$(C–H)	0	0.99
$n_pO^3 \rightarrow$BD*(R group)	—	3.24	2.07	—	—	2.98	2.28	—	—	—	—	—
$n_pO^1 \rightarrow \sigma^*$(P–O^3)	0	0	0	0	1.59	1.46	1.40	1.46	1.31	—	—	—
$n_pO^1 \rightarrow \sigma^*$(P–O$_2$)	4.07	4.04	3.95	4.15	5.22	4.89	4.73	5.22	4.75	—	—	—
$n_pO^3 \rightarrow \sigma^*$(O^1–H)	4.46	5.84	6.03	4.19	—	—	—	—	—	—	—	—

[a] Interactions < 0.5 kcal mol^{-1} are shown as zero; σ* orbitals are approx. sp^2 on O and involve d-orbitals on P; BD*(R) includes all antibonding orbitals associated with the R group (CF_2H or CH_3). [b] ⊥ CHO in equatorial plane; ∥ CHO in apical plane. [c] Donation to σ*(C=O) orbital.

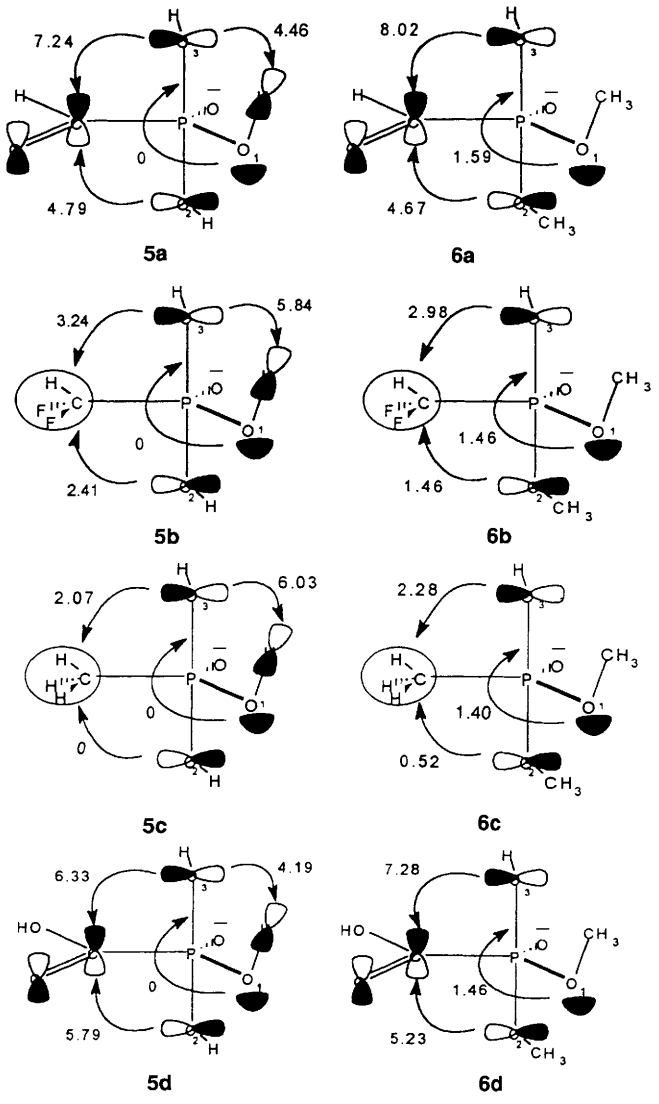

Fig. 2 Significant charge-transfer interactions from NBO analysis of RHF/6-31G*//6-31G* calculations on pentacoordinate phosphorane intermediates, **5a–d**, and **6a–d**, as detailed in Table 2 and the text, represented graphically

hydrolysis in $^{18}OH_2$, of zero or incomplete label incorporation at the carbonyl carbon and complete incorporation at phosphorus in the product **10**, suggests a simple mechanism involving direct in-line nucleophilic displacement on phosphorus (Scheme 2). However, this mechanism relies on the

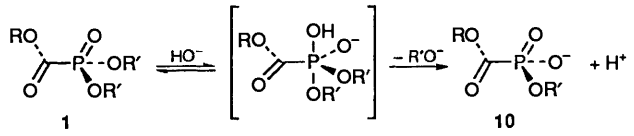

Scheme 2

electron-withdrawing effect of the alkoxycarbonyl substituent alone to activate the system towards hydrolysis. The electron-withdrawing ability of a difluoromethyl substituent is approximated as comparable to that of the alkoxycarbonyl group by Taft parameters,[29] yet P–O bond cleavage in **1a** and **1b** proceeds 10^3–10^5 times faster than hydrolysis of **3**. We have suggested that neighbouring-group participation by the α-carbonyl group, either *via* hydrate formation or simply through stereoelectronic interactions with the carbonyl moiety, may account for the experimentally observed rate enhancement.[7a]

Comparison with $B_{AC}2$ *and* S_N2 *Reactions Adjacent to an* α-*Carbonyl Group.*—Detailed kinetic analysis by Bruice and co-workers, on hydroxide-dependent hydrolysis of aryl esters, allows construction of a Taft plot for a series of substituted carboxylate esters including the ethyl oxalate ester (Fig. 3).[30] The excellent correlation includes the oxalate, which clearly shows no special reactivity. A similar good correlation is shown on analysis of the data for base-catalysed hydrolysis of a large series of methyl and ethyl carboxylate esters compiled by Guthrie.[31] In particular, although the second-order rate constant reported for diethyl oxalate is 8 × 10^4 greater than for ethyl acetate, it is only three times greater than that for ethyl difluoroacetate. The influence of the α-carbonyl substituent on reactivity towards nucleophilic substitution at acyl carbon is thus greatly diminished relative to its influence on reaction at phosphorus.

It is reported in the literature that S_N2 substitution of ethoxycarbonylchloromethane by iodide in acetone proceeds at a rate 6.8 × 10^2 times faster than that of ethyl chloride.[32] This observed rate enhancement (the analogous rate enhancement in nucleophilic substitution at phosphorus is 10^6 from comparison of hydrolysis rates for **1c** and **2b**) has prompted a series of theoretical papers directed at elucidating the mechanism by which an α-keto substituent accelerates displacement of halide from an adjacent sp^3 carbon. Among other studies,[33] Shaik has employed the intersystem-crossing, valence bond model;[34] Wolfe and co-workers have used a perturbational molecular orbital approach;[35] and Bach and co-workers have made reference to frontier molecular orbitals.[36]

In particular, Kost and co-workers have provided a model for an S_N2 reaction in which rate acceleration is provided by the stabilizing interaction of π-acceptor substituents with the HOMO-1 orbital corresponding to the reaction coordinate in the transition state[37] (Scheme 3). The explanation for enhanced S_N2 reactivity provided, rests on the proposal of a stabilizing interaction in the pentacoordinate transition state between the carbonyl and CH_2X_2 molecular fragments, termed σ–π conjugation.[33] The torsional energy barrier of 11 kcal mol^{-1} [for rotation about the C–C bond of $HC(O)CCl_2H_2^-$] has been provided as evidence for this stereoelectronic effect (Scheme 1).[36] Phosphoranes **9a,b** are comparable to the S_N2 transition-state models used by Wolfe *et al.* [$HC(O)CF_2H_2^-$] and by Bach *et al.* [$HC(O)CCl_2H_2^-$] (Scheme 1).[35,36] A substantial barrier to rotation about the P–C bond of **9a, b** might be predicted on the basis of the proposed stereoelectronic effects at pentacoordinate carbon. However, the difference in energy between the dihalophosphorane conformers is very small (Scheme 1). In both compounds, at each level of calculation, there is no clear energy advantage for the formyl group to rest in the equatorial

Table 4 Geometrical parameters and charge-transfer stabilization energies (kcal mol^{-1}) for tetrahedral intermediates

	7a	7b
d(C–C)/Å	1.530	1.551
d(C–O^5)/Å	1.446	1.435
d(C–O^6)/Å	1.416	1.418
d(C–O^7)/Å	1.281	1.275
d(C=O)/Å	1.193	1.194
∠O^3CR	120.19	119.07
∠O^5CC	104.36	106.53
∠O^6CC	106.58	103.89
τ(HO^5CC)	107.44	119.61
τ(HOC^2=O)	2.22	—
τ(CO^6CC)	195.77	193.20
τ(O^5CCO_3)	133.45	121.43
$n_p(O^5)\rightarrow\pi^*$(C=O)	3.07	2.02
$n_p(O^5)\rightarrow\pi^*$(C–O^6)	0.80	—
$n_p(O^6)\rightarrow\pi^*$(C–O^4)	0	0.85
$n_p(O^6)\rightarrow\pi^*$(C–O^5)	17.77	16.62
$n_p(O^7)\rightarrow\pi^*$(C=O)	0.58	4.87

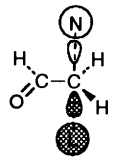

Scheme 3 HOMO-1 π-donor (N = nucleophile, L = leaving group)

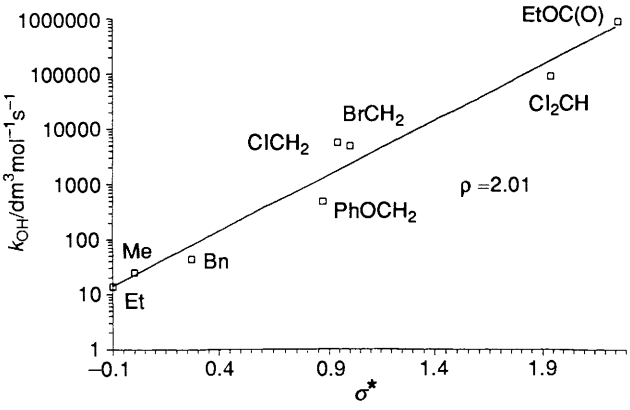

Fig. 3 Taft plot of second-order rate constants for hydroxide-dependent hydrolysis of *o*-nitrophenyl carboxylate esters at 30 °C, derived from literature data (ref. 30)

rather than the apical plane. Speculation on the cause of this disagreement is not justified because of the different level of calculation and geometry restrictions used in the published calculations on pentacoordinate carbon.* Full relaxation of **9a** with the formyl group in the apical plane does incur substantial geometrical deformation.

Rotational Profiles for α-Carbonyl Phosphoranes.—Energy profiles for rotation about the P–C bonds of phosphoranes **8** and **6a** were calculated (Fig. 1). The energy minima correspond to the conformers with the formyl group in the equatorial plane, which is consistent with the presence of a similar stereoelectronic interaction, between the formyl and $PO_4H_2Me^-$ fragments, to that proposed in pentacoordinate carbon species, *vide supra*. Geometrical changes in **6a** are also consistent with such a stereoelectronic interaction. The most significant change on rotation of the formyl group from the equatorial to apical plane is elongation of the P–C bond by 0.06 Å. However, since steric interactions will be maximized with the formyl group in the apical plane, this evidence for a stereoelectronic effect is not unambiguous.

Natural Bond Orbital Analysis of Stereoelectronic Interactions.—For phosphoranes **5a,d**, **6a,d**, the carbonyl moiety rests at the equatorial position and in the equatorial plane in all stationary points located. All phosphoranes possess a distorted TBP structure with apical O–P–O bond angles less than 180° (Table 2). Second-order perturbation theory analysis of the Fock matrix derived from the NBO basis yields stabilization energies for pairwise charge-transfer interactions categorized as geminal, vicinal and remote. Remote interactions between the apical and equatorial substituents, in addition to geminal interactions involving equatorial oxygen donors (including the GT effect) are represented in Table 2 and Fig. 2. In both **5a** and **5b** there is clearly a substantial stabilization deriving from electron donation from the apical oxygen π-type lone pair to the equatorial σ*(H–O) orbital. This stabilization may be categorized as intramolecular hydrogen-bonding. In contrast, stabilizing remote interactions with the equatorial carbon substituent are of much greater magnitude for the α-carbonyl phosphorane **5a** than the fluoromethyl phosphorane **5b**. Charge-transfer stabilization involving both apical oxygens, of the type $n_p(O)\rightarrow\pi^*(C{=}O)$, is worth 12.2 kcal mol^{-1}, whereas no such stabilization is possible for the fluoromethyl phosphorane. Using this analysis, the sum of such $n_p(O)$ apical donor interactions with the equatorial carbon substituent, stabilizes the α-carbonyl phosphorane over the fluoromethyl phosphorane by almost 7 kcal mol^{-1}. Study of vicinal interactions indicates the absence of any evidence for the GT effect, which is specifically stated to derive from antiperiplanar $n(O)_{equatorial}\rightarrow\sigma^*(P{-}O_{apical})$ orbital mixing.[8] In fact stabilizing *synperiplanar* $n(O)\rightarrow\sigma^*(P{-}O)$ interactions are observed, contrary to the GT hypothesis (Table 2).

A similar comparison may be made in the methoxyphosphorane series (**6**) between the α-carbonyl phosphorane (**6a**) and fluoromethyl phosphorane (**6b**) (Fig. 2). Again significant $n_p(O)\rightarrow\pi^*(C{=}O)$ stabilization is observed. In this case, of course, no intramolecular hydrogen bonding, of the type $n(O)\rightarrow\sigma^*(H{-}O)$, is possible, but the C–H antibonding orbitals are effective acceptors. Indeed, stabilizing vicinal interactions of methoxy n(O) donor orbitals with the σ*(C–H) and π*(C–H) orbitals of the methyl group provide an explanation for the observed, enhanced stabilization of TBP structures bearing an apical methoxy rather than hydroxy ligand in calculations *in vacuo*.[12a] The GT effect interactions are again observed to be minor (Table 2). Methyl phosphorane **6c** and hydroxycarbonyl phosphorane **6d** manifest similar charge-transfer interactions to those observed for **6b** and **6a**, respectively (Fig. 2, Table 2).

It is useful to examine the effect of rotation about the P–C bond on charge-transfer interactions, from NBO analysis, for both dichlorophosphorane **9a** and phosphorane **6a**. The large $n(O)_{apical}\rightarrow\pi^*(C{=}O)$ stabilization (13 kcal mol^{-1}) observed in **6a** with the carbonyl moiety in the equatorial plane is lost completely on rotation about the P–C bond. With the carbonyl moiety in the apical plane, there is in its place, a small $n(O)_{apical}\rightarrow\sigma^*(C{=}O)$ interaction worth only 3 kcal mol^{-1} (Table 2). The situation in the dichlorophosphorane is somewhat different; a smaller $n(Cl)\rightarrow\pi^*(C{=}O)$ stabilization (7.4 kcal mol^{-1}) is replaced by $n(Cl)\rightarrow\sigma^*(C{=}O)$ (2 kcal mol^{-1}) and $n(Cl)\rightarrow\sigma^*(C{-}H)$ (1 kcal mol^{-1}) interactions. This data correlates well with the calculated small destabilization of the dichlorophosphorane compared with phosphorane **6a** on rotation of the carbonyl moiety out of the equatorial plane (Scheme 1, Fig. 1).

A more rigorous treatment of charge-transfer stabilization using NBO analysis involves deletion of each individual interaction then recalculation of the molecular energy. In addition, quantitative comparison of all interactions between the two pairs of model compounds **5a,b** and **6a,b** should be attempted rather than a selective treatment (as in Table 2, Fig. 2). From this analysis, it may be seen that although many individual interactions are of larger magnitude than those discussed above (Table 2), these generally cancel (Table 3). Thus comparison of contributions to stabilization of the carbonyl phosphoranes **5a** and **6a** over the fluoromethyl phosphoranes **5b** and **6b**, respectively, yields the same three qualitative conclusions as were drawn from the simple second-order perturbation analysis: (1) intramolecular hydrogen bonding

* Kost and Aviram make the important observation of increased 'S_N1-like' character, as indicated by increased apical bond lengths in the pentacoordinate transition state, in the presence of stabilizing orbital interactions with α-carbonyl substituents. This trend is not mirrored in the phosphoranes **6a–d** (Table 2). Contrasts also exist in the experimental data: (1) the rate enhancement for substitution at phosphorus is substantially larger, (2) the observed rapid rate of S_N2 reactions at the benzyl carbon has been rationalized by a similar stereoelectronic effect to that suggested for S_N2 reaction α to a carbonyl group,[33,36] whereas phenyl phosphonate esters (comparable in this case to benzyl halides) undergo hydroxide-dependent hydrolysis barely faster than methyl phosphonate esters.

[$n(O_{apical})\rightarrow\sigma^*(H-O)$] stabilizes both carbonyl and fluoromethyl phosphoranes (**5a,b**) by 4.0–5.2 kcal mol^{-1}; (2) the influence of the GT effect is minor, ranging from 01–1.1 kcal mol^{-1}; (3) the major contribution to stabilization of the α-carbonyl phosphoranes over fluoromethyl phosphoranes is an $n_p(O)\rightarrow\pi^*(C=O)$ interaction contributing 3.9–5.4 kcal mol^{-1} (Table 3).

Influence of Calculated Stereoelectronic Effects on Reaction Rate.—α-Carbonyl phosphoranes **5a,d** and **6a,d** model the pentacoordinate intermediates in hydrolysis of the PFA esters **1** (Scheme 2). Similarly **5b** and **6b** model reaction of difluoromethyl phosphonate **3**; and **5c** and **6c** model reaction of methyl phosphonate **2**. The most significant comparison is between the stabilizing charge-transfer interactions calculated for the α-carbonyl phosphoranes (**5a,d**, **6a,d**) and difluoromethyl phosphoranes (**5b**, **6b**); these model intermediates resulting from reaction of the two activated phosphonates, α-carbonyl and difluoromethyl, respectively. Any significant stabilization of the α-carbonyl phosphorane represents a possible cause of the observed rate difference. Simple NBO analysis indicates that the pentacoordinate intermediates in hydrolysis of α-carbonyl phosphonates are stabilized by ≈6–8 kcal mol^{-1} relative to intermediates involved in hydrolysis of difluoromethyl phosphonates as a result of $n_p(O)\rightarrow\pi^*(C=O)$ charge transfer (Table 2). More rigorous NBO analysis (Table 3) yields a stabilization energy of 4–5 kcal mol^{-1}. The high energy pentacoordinate intermediate in substitution at phosphorus will resemble the transition state for this reaction. Thus if the calculated stabilization energy, of 4–5 kcal mol^{-1}, is applied to the transition state for hydrolysis, a rate enhancement of 10^3–10^5 for hydrolysis of **1a** over **3** is predicted. The relative energy differences between the tetrahedral ground states (**4a–d**) and pentacoordinate intermediates (**6a–d**) yield a further measure of the special stabilization of the pentacoordinate over the tetrahedral state, attributed to the α-carbonyl substituent, and give an estimate of relative barriers to reaction (Fig. 4). The calculated relative energy differences, for the series of four phosphonates, correlate well with the observed relative reaction rates in solution for α-carbonyl, difluoromethyl and methyl phosphonates.

Calculations on Tetrahedral Intermediates in Ester Oxalate Hydrolysis.—Since the rate of hydroxide-dependent hydrolysis of ethyl *o*-nitrophenyl oxalate does not lie off the Taft plot for *o*-nitrophenyl esters (Fig. 3), it may be predicted that a similar $n_p(O)\rightarrow\pi^*(C=O)$ interaction in the tetrahedral intermediate and transition state does not assist hydrolysis of oxalate esters. NBO analysis on models for tetrahedral intermediates involved in oxalate ester hydrolysis (**7a,b**) demonstrate much reduced interactions from $n_p(O)\rightarrow\pi^*(C=O)$ donation (Table 4). Stabilizing interactions of 3.1 and 2.0 kcal mol^{-1}, for **7a** and **7b**, respectively, compare with stabilization of 12–12.5 kcal mol^{-1} for phosphorus intermediates calculated in the same manner. In fact, the NBO analysis of **7a,b** is dominated by a vicinal $n_p(O)\rightarrow\sigma^*(C-O)$ interaction analogous to an anomeric effect. The diminished $n_p(O)\rightarrow\pi^*(C=O)$ remote interaction is compatible with the decreased orbital overlap inherent in a tetrahedral rather than a pentacoordinate geometry. Indeed, in the pentacoordinate state the angle at the reaction centre is reduced from 90° to increase overlap still further. This structural distortion is observed both in S_N2 transition states[37] and the phosphorane intermediates in this study (Table 2). In the methoxy phosphorane series (**6a,b,d**), $\angle O_{apical}PC$ averages at 82.6° for α-carbonyl derivatives in comparison to 86.0° for the methyl phosphorane **6b**. Bond angles in the hydroxy series (**5a–d**) show a similar trend, but are influenced by intramolecular hydrogen bonding. Increased structural flexibility in the transition states for both phosphonate and carboxylate ester hydrolysis provides scope for greater orbital overlap than in the trigonal bipyramidal and tetrahedral intermediates themselves. Further calculations, in particular on transition-state models for oxalate hydrolysis, are warranted.

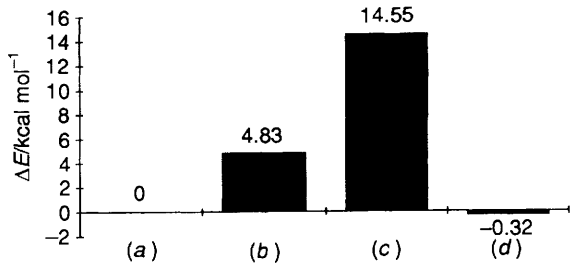

Fig. 4 Relative energies of pentacoordinate phosphoranes (**6a–d**) to tetrahedral ground states (**4a–d**), calculated as $\Delta E = [E(\mathbf{6}) - E(\mathbf{4})] - [E(\mathbf{6a}) - E(\mathbf{4a})]$, *i.e.*, $[E(\mathbf{6a}) - E(\mathbf{4a})]$ is set as zero. ΔE provides an estimate of the special stabilization of the α-carbonyl species in the pentacoordinate state over the tetrahedral ground state. Comparative values at the MP2/6-31G*//HF/6-31G* level for **6a** and **6d** are reversed from −0.3 to +0.2 kcal mol^{-1}.

Conclusions

Stereoelectronic Effects at Phosphorus.—Molecular orbital calculations *in vacuo* reveal significant dependence of energy on torsion angle in pentacoordinate phosphoranes. Destabilization from electrostatic interactions may result in the minimization of these interactions being the dominant factor in determining conformational energy. Identification of causal factors for observed stereoelectronic phenomena requires localization of stabilizing orbital interactions. NBO analysis of phosphonate pentacoordinate intermediates reveals a number of such interactions, but a clear contraindication for the $n(O)\rightarrow\sigma^*(P-O)$ GT effect.† The most significant stabilizing charge-transfer interactions located are: (1) intramolecular, $n_p(O)\rightarrow\sigma^*(O-H)$, hydrogen-bonding interactions which dominate in the hydroxyphosphoranes (*e.g.*, **5**); and (2) $n_p(O)\rightarrow\pi^*(C=O)$ interactions stabilizing the pentacoordinate state and supporting stereoelectronic acceleration as the cause of the observed enhanced rate of nucleophilic substitution of α-carbonyl phosphonates. The importance of such intramolecular charge-transfer interactions, calculated in the gas phase, to reactions in aqueous solution is, of course, problematic. The calculated gas-phase stabilization energies (Tables 2 and 3) and estimated energy barriers (Fig. 4) for addition of hydroxide to the four phosphonates, in this present study, correlate well with trends in reactivity for the three phosphonates **1**, **2** and **3**, from experimental observations in solution. Nevertheless, the question as to whether the numerous charge-transfer and electrostatic interactions with solvent may overwhelm similar intramolecular interactions remains. Calculations are being extended to include full reaction energy profiles including solvation corrections.

Influence of the α-Carbonyl Substituent on Reactivity.—Molecular orbital calculations support an explanation for the large rate enhancement observed in the hydrolysis of α-carbonyl phosphonates based on stereoelectronic interactions. Although this stereoelectronic effect provides a satisfying rationale for phosphonate reactivity, the NBO analysis, in itself, does not rule out the involvement of bridged species involving covalent

† A similar torsional energy dependence *in vacuo* to that first noted by Gorenstein's group in calculations on phosphoranes and leading to an extensive theory of reactivity,[8] is also found in sulfuranes: the cause in sulfuranes has been defined as intramolecular hydrogen-bonding.[38]

interaction with the carbonyl carbon.[39] The $n_p(O) \rightarrow \pi^*(C{=}O)$ stabilizing interactions between nucleophile or leaving group and the equatorial carbonyl moiety, that form the basis of this stereoelectronic effect, are facilitated in reaction intermediates by the pentacoordinate TBP geometry. This mechanism of stereoelectronic acceleration of nucleophilic substitution at phosphorus bears comparison to stereoelectronic effects proposed for S_N2 reaction at carbon. Conversely, the diminished $n_p(O) \rightarrow \pi^*(C{=}O)$ interaction observed in the tetrahedral, tetracoordinate state predicts and is compatible with the absence of such stereoelectronic acceleration in nucleophilic substitution at acyl carbon. Clearly, the increased orbital overlap in the more crowded pentacoordinate state is a major factor in controlling the magnitude of stereoelectronic interactions between substituents.

Catalysis of Nucleophilic Substitution at Phosphorus.—The large rate enhancement observed in hydrolysis of PFA triesters has required determination of a novel mechanism for acceleration of nucleophilic substitution at phosphorus. Systems in which rate enhancements are observed are frequently employed as models for enzymic catalysis, in particular in phosphoryl transfer.[6] Extrapolation of our conclusions on PFA ester reactivity would require the presence of an intermolecular charge-transfer interaction to provide catalysis of reaction at phosphorus, either in assistance of approach of the nucleophile or loss of the leaving group. Clearly, the problem envisaged would be providing sufficient orbital overlap in an intermolecular interaction.

Supplementary Material Available.—Cartesian coordinates for stationary points corresponding to compounds **5a–d**, **6a–d**, **9a** (4 pages) have been deposited with the British Library, Sup. No. 57003. For details of the Supplementary Publications Scheme see 'Instructions for Authors (1994)', *J. Chem. Soc., Perkin Trans. 2*, 1994, issue 1.

Acknowledgements

The donors of the Petroleum Research Fund administered by the American Chemical Society are thanked for financial support.

References

1 F. H. Westheimer, *Science*, 1987, **235**, 1173.
2 C. Helene and J. J. Toulme, *Biochem. Biophys. Acta*, 1990, **1049**, 99.
3 S. Freeman, S. J. Pollack and J. R. Knowles, *J. Am. Chem. Soc.*, 1992, **114**, 377.
4 J. E. Chambers and P. E. Levi, *Organophosphates: Chemistry, Fate and Effects*, Academic Press, San Diego, California, 1987.
5 G. R. J. Thatcher and R. Kluger, *Adv. Phys. Org. Chem.*, 1989, **25**, 99.
6 J. Chin, *Acc. Chem. Res.*, 1991, **24**, 145.
7 (*a*) E. S. Krol and G. R. J. Thatcher, *J. Chem. Soc., Perkin Trans. 2*, 1993, 793; (*b*) E. S. Krol, J. M. Davis and G. R. J. Thatcher, *J. Chem. Soc., Chem. Commun.*, 1991, 118.
8 For recent reviews see (*a*) papers in *The Anomeric Effect and Associated Stereoelectronic Effects*, ed. G. R. J. Thatcher, ACS Symposium Series No. 539, ACS, Washington DC, 1993; (*b*) E. Juaristi and G. Cuevas, *Tetrahedron*, 1992, **48**, 5019.
9 For example, W. N. Setzar and W. G. Bentrude, *J. Org. Chem.*, 1991, **56**, 7212; R. W. Warrent, C. N. Caughlin, J. H. Hargis, K. C. Yee and W. G. Bentrude, *J. Org. Chem.*, 1987, **43**, 4266.
10 J.-M. Lehn and G. H. Wipff, *J. Chem. Soc., Chem. Commun.*, 1975, 800.
11 J. P. Foster and F. Weinhold, *J. Am. Chem. Soc.*, 1980, **102**, 7211; A. E. Reed and F. Weinhold, *J. Chem. Phys.*, 1983, **78**, 4066; A. E. Reed, R. B. Weinstock and F. Weinhold, *J. Chem. Phys.*, 1985, **83**, 735; J. E. Carpenter and F. Weinhold, *J. Mol. Struct. (Theochem.)*, 1988, **169**, 41.
12 For example, A. E. Reed and P. v. R. Schleyer, *Inorg. Chem.*, 1988, **27**, 3969; see also P. A. Petillo and L. E. Lerner, *The Anomeric Effect and Associated Stereoelectronic Effects*, ed. G. R. J. Thatcher, ACS Symposium Series No. 539, 156–175, ACS, Washington DC, 1993.
13 S. A. Bone, S. Trippett and P. J. Whittle, *J. Chem. Soc., Perkin Trans. 1*, 1977, 80.
14 (*a*) P. Wang, Y. Zhang, R. Glaser, A. E. Reed, P. v. R. Schleyer and A. Streitwieser, *J. Am. Chem. Soc.*, 1991, **113**, 55; R. S. McDowell and A. Streitwieser, *J. Am. Chem. Soc.*, 1985, **107**, 5849; (*b*) C. J. Cramer, *Chem. Phys. Lett.*, 1993, **202**, 297.
15 Summarized in D. G. Gorenstein, *Chem. Rev.*, 1987, 1047.
16 (*a*) J. W. Storer, T. Uchimara, K. Tanabe, M. Uebajasi, S. Nishikawa and K. Taira, *J. Am. Chem. Soc.*, 1991, **113**, 5216; (*b*) K. Taira, T. Uchimara, K. Tanabe, M. Uebayasi, S. Nishikawa, *Nucleic Acids Res.*, 1991, **19**, 2747.
17 (*a*) A. J. Kirby, *The Anomeric Effect and Related Stereoelectronic Effects at Oxygen*, Springer, Berlin, 1983; (*b*) A. J. Kirby and N. H. Williams, *The Anomeric Effect and Associated Stereoelectronic Effects*, ed. G. R. J. Thatcher, ACS Symposium Series No. 539, 55–69, ACS, Washington DC, 1993.
18 P. Deslongchamps, *Stereoelectronic Effects in Organic Chemistry*, Pergamon, Oxford, 1983; P. Deslongchamps, *The Anomeric Effect and Associated Stereoelectronic Effects*, ed. G. R. J. Thatcher, ACS Symposium Series No. 539, 26-54, ACS, Washington DC, 1993.
19 G. R. J. Thatcher, *The Anomeric Effect and Associated Stereoelectronic Effects*, ed. G. R. J. Thatcher, ACS Symposium Series No. 539, 6-25, ACS, Washington DC, 1993.
20 (*a*) R. Kluger and F. H. Westheimer, *J. Am. Chem. Soc.*, 1969, **91**, 4143; (*b*) R. Kluger and G. R. J. Thatcher, *J. Am. Chem. Soc.*, 1985, **107**, 6006; (*c*) R. Kluger and G. R. J. Thatcher, *J. Org. Chem.*, 1986, **51**, 207; (*d*) R. Kluger and S. Taylor, *J. Am. Chem. Soc.*, 1990, **112**, 6669.
21 F. H. Westheimer, *Special Publication No. 8*, The Chemical Society, London, 1957; D. A. Usher, E. A. Dennis and F. H. Westheimer, *J. Am. Chem. Soc.*, 1965, **87**, 2320; ref. 12(*b*), p. 166.
22 (*a*) F. Ramirez and N. B. Desai, *J. Am. Chem. Soc.*, 1960, **82**, 2652; (*b*) S. D. Taylor and R. Kluger, *J. Am. Chem. Soc.*, 1992, **114**, 3067; (*c*) J. A. Gerlt, F. H. Westheimer and J. M. Sturtevant, *J. Biol. Chem.*, 1975, **250**, 5059; (*d*) A. Dejaegere and M. Karplus, *J. Am. Chem. Soc.*, 1993, **115**, 5316.
23 GAUSSIAN 92, Revision C, M. J. Frisch, G. W. Trucks, M. Head-Gordon, P. M. W. Gill, M. W. Wong, J. B. Foresman, B. G. Johnson, H. B. Schlegel, M. A. Robb, E. S. Replogle, R. Gomperts, J. L. Andes, K. Raghavachari, J. S. Binkley, C. Gonzalez, R. L. Martin, D. J. Fox, D. J. DeFrees, J. Baker, J. J. P. Stewart and J. A. Pople, Gaussian Inc., Pittsburgh, PA, 1992.
24 C. M. Breneman and K. B. Wiberg, *J. Comput. Chem.*, 1990, **11**, 361.
25 SPARTAN v.3.0, Wavefunction Inc. 18401 Von Karman, #210, Irvine, CA, 92715.
26 W. J. Pietro, M. M. Francl, W. J. Hehre, D. J. DeFrees, J. A. Pople and J. S. Binkley, *J. Am. Chem. Soc.*, 1982, **104**, 5039; T. Clark, J. Chandrasekhar, G. W. Spitznagel and P. v. R. Schleyer, *J. Comput. Chem.*, 1983, **4**, 294; M. J. Frisch, J. A. Pople and J. S. Binkley, *J. Chem. Phys.*, 1984, **80**, 3265.
27 G. R. J. Thatcher and A. S. Campbell, *J. Org. Chem.*, 1993, **58**, 2272.
28 C. Liang, C. S. Ewig, T. R. Stouch and A. T. Hagler, *J. Am. Chem. Soc.*, 1993, **115**, 1537.
29 D. D. Perrin, pK_a *Prediction for Organic Acids and Bases*, Chapman & Hall, London, 1981.
30 B. Holmquist and T. C. Bruice, *J. Am. Chem. Soc.*, 1969, **91**, 2982; T. C. Bruice and B. Holmquist, *J. Am. Chem. Soc.*, 1967, **89**, 4028.
31 J. P. Guthrie and P. A. Cullimore, *Can. J. Chem.*, 1980, **58**, 1281.
32 J. Hine, *Physical Organic Chemistry*, 2nd edn., pp. 175–180, McGraw-Hill, New York, 1962.
33 F. Carrion and M. J. S. Dewar, *J. Am. Chem. Soc.*, 1984, **106**, 3531; A. Pross, K. Aviram, R. C. Klix, D. Kost, R. D. Bach, *Nouv. J. Chim.*, 1984, **8**, 711.
34 S. S. Shaik, *J. Am. Chem. Soc.*, 1983, **105**, 4359.
35 S. Wolfe, D. J. Mitchell and H. B. Schlegel, *Can. J. Chem.*, 1982, **60**, 1291.
36 R. D. Bach, B. A. Coddens and G. J. Wolber, *J. Org. Chem.*, 1986, **51**, 1030.
37 D. Kost and K. Aviram, *J. Am. Chem. Soc.*, 1986, **108**, 2006.
38 D. R. Cameron and G. R. J. Thatcher, *The Anomeric Effect and Associated Stereoelectronic Effects*, ed. G. R. J. Thatcher, ACS Symposium Series No. 539, 256–276, ACS, Washington DC, 1993.
39 I. Lee, C. S. Shim, S. Y. Chung and H. W. Lee, *J. Chem. Soc., Perkin Trans. 2*, 1988, 975.

Paper 3/07342D
Received 13*th December* 1993
Accepted 18*th January* 1994